J. Fluid Mech. (1972), *vol.* 56, *part* 4, *pp.* 753–774
Printed in Great Britain

Compressible corner flow

By BERNARD C. WEINBERG† AND STANLEY G. RUBIN

Polytechnic Institute of Brooklyn,
Preston R. Bassett Research Laboratory, Farmingdale, New York

(Received 5 May 1972)

The viscous compressible flow in the vicinity of a right-angle corner, formed by the intersection of two perpendicular flat plates and aligned with the free stream, is investigated. In the absence of viscous–inviscid interactions and imbedded shock waves, a theory is developed that is valid throughout the subsonic and supersonic Mach number range. Within this limitation and the additional assumptions of unit Prandtl number and a linear viscosity–temperature law, a consistent set of governing equations and boundary conditions is derived. The method of matched asymptotic expansions is applied in order to distinguish the relevant regions in the flow field.

In the corner region the Crocco integral is shown to apply, even for a three-dimensional flow field. The equations governing the flow in the corner layer consist of four coupled nonlinear elliptic partial differential equations of the Poisson variety. Since they do not lend themselves to analytic solution, numerical methods are employed. Two such methods used here are the Gauss–Seidel explicit technique and the alternating direction implicit method. The merits of both techniques are discussed with regard to convergence rate, accuracy and stability. The calculations show that in cases where the Gauss–Seidel method fails to give converged solutions, owing to instability, the alternating direction implicit method does provide converged solutions. However, in cases where both methods are convergent, there is no appreciable difference in convergence rates. The numerical calculations were done on a CDC 6600 computer.

Results of calculations are presented for representative compressible-flow conditions. The extent of the corner disturbance is controlled by the Mach number and wall temperature ratio in a manner analogous to the two-dimensional boundary layer. A swirling motion is noted in the corner layer which is influenced to a great extent by the asymptotic cross-flow profiles. The skin-friction coefficient is shown to increase monotonically from zero at the corner point to its asymptotic two-dimensional value. For cold wall cases, this value is approached more rapidly. The asymptotic analysis indicates that for even colder wall cases, not considered here, an overshoot is possible.

† Present address: Department of Fluid and Heat Transfer, Negev University, Beer-Sheva, Israel.

1. Introduction

The three-dimensional viscous interaction in the neighbourhood of the intersection of two perpendicular surfaces is of fundamental interest. Since this geometry manifests itself in many practical configurations, such as wing fuselage junctures and wing-fin assemblies, a knowledge of the flow field in the vicinity of the intersection is essential for a complete understanding of the physical nature of the problem.

The viscous flow along a corner has previously been investigated in great detail for the limiting cases of incompressible and hypersonic flow. The existing theoretical and experimental investigations (see e.g. the review by Bloom, Rubin & Cresci 1970) have discussed the heat transfer and pressure behaviour. For high-speed flow, overshoots have been found. They do not appear in the incompressible case. For the cross-flow velocity, a swirling motion has been obtained for low-speed flows, with vortex formation possible in high-speed flows. Unlike high Reynolds number viscous flows over bodies with small transverse curvature (for which two-dimensional boundary-layer theory is generally applicable), the corner geometry is inherently three-dimensional.

It is generally not realized that the viscous flow along a corner, even asymptotically far downstream from the leading edge, constitutes a 'strong' interaction in the sense that the boundary-layer induced perturbations of the inviscid flow field must affect even the lowest-order analysis for the viscous three-dimensional flow in the immediate corner region. Furthermore, the proper analytic model of the flow can be obtained only when these boundary-layer displacement effects are taken into account.

Rubin (1966) was the first to formulate the low-speed corner problem correctly; subsequently, Pal & Rubin (1971) and Rubin & Grossman (1971) evaluated the asymptotic characteristics and numerical solutions for the incompressible corner region. Their results show that the skin-friction coefficient at the wall increases monotonically from zero at the corner point to its asymptotic two-dimensional value within three to four two-dimensional flat-plate boundary-layer thicknesses. A crosswise influx is also noted, and a swirling motion is found to exist in the corner layer.

Published results for the hypersonic case where viscous–inviscid shock interactions occur indicate the presence of overshoots in heat transfer and skin friction in the vicinity of the corner intersection as well as the formation of streamwise vortices. Thus, a fundamental difference exists between the low-speed and hypersonic corner interaction problems. Subsonic and low supersonic flows were treated by Bloom & Rubin (1961) by integral methods. Their solutions were not entirely satisfactory, as they did not consider the complete cross-flow behaviour.

In this paper the effects of compressibility on the corner-layer analysis are considered. The governing equations, the associated boundary conditions, and the numerical solutions are presented. The theory applies for the entire Mach number range (incompressible to supersonic) in the absence of viscous–inviscid interactions. A boundary-layer type of analysis is employed in a manner similar to the incompressible-flow analysis of Rubin (1966). In this regard, the

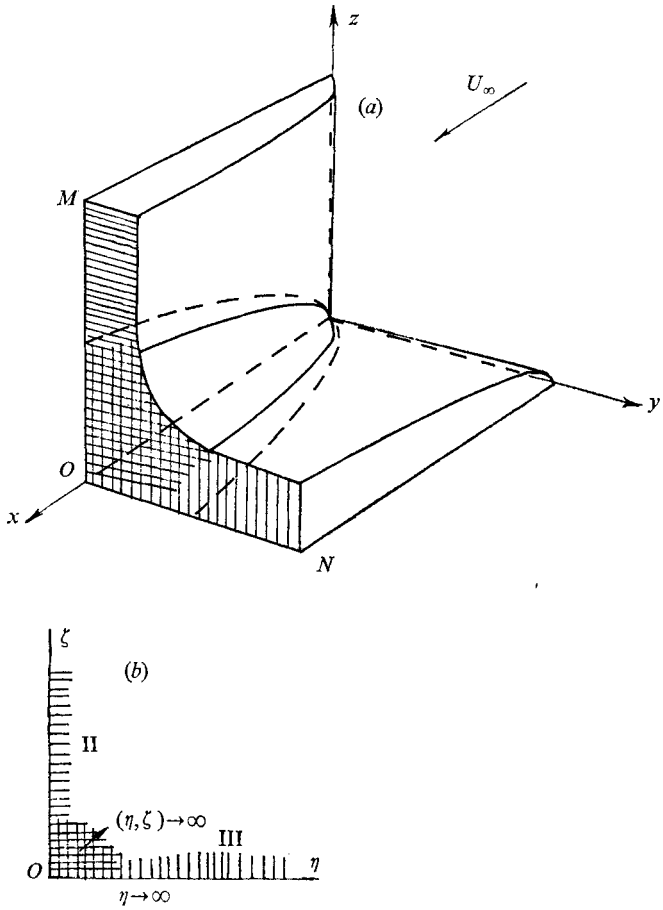

FIGURE 1. (*a*) Corner-flow geometry. (*b*) Section *MON* (outer flow co-ordinates x, y, z).

Region	Boundary-layer similarity co-ordinates	
II	$\bar{\eta} = \bar{Y}/(2x)^{\frac{1}{2}}$,	$\bar{Y} = Re^{\frac{1}{2}} \int_0^y \rho_{2D}\, dy$
III	$\bar{\zeta} = \bar{Z}/(2x)^{\frac{1}{2}}$,	$\bar{Z} = Re^{\frac{1}{2}} \int_0^z \rho_{2D}\, dz$
	$\eta = y\, Re^{\frac{1}{2}}/(2x)^{\frac{1}{2}}$,	$\zeta = z\, Re^{-\frac{1}{2}}/(2x)^{\frac{1}{2}}$

solutions are valid several boundary-layer thicknesses downstream of the leading edge.

Consider the viscous compressible flow along a right-angle corner formed by the intersection of two semi-infinite flat plates. The schematic diagram (figure 1) depicts the flow geometry. Various viscous and inviscid regions are distinguished. The undisturbed velocity vector U_∞ is directed along x. The relevant co-ordinates defining the different regions are given in table 1. Here $Re = \rho_\infty U_\infty L/\mu_\infty$ and ρ_{2D} is the two-dimensional density, defined explicitly in § 3.

The laterally extending boundary layers, shown singly cross-hatched, are two-dimensional far from the corner (i.e. $z \to \infty$, $\bar{\eta}$ finite), and quasi-two-dimensional

Potential flow	Boundary layer (II)	Corner layer
$x > 0, y > 0, z > 0$	$x > 0, \bar{Y} > 0, z > 0$	$x > 0, Y > 0, Z > 0$
$x = O(1)$	$\bar{\eta} = \bar{Y}/(2x)^{\frac{1}{2}} = O(1)$	$\eta = Y/(2x)^{\frac{1}{2}} = O(1)$
$y = O(1)$	$\bar{Y} = \left\{\int_0^Y \rho_{2D}\, d\xi\right\} Re^{\frac{1}{2}}$	$\zeta = Z/(2x)^{\frac{1}{2}} = O(1)$
$z = O(1)$		$Y = yRe^{\frac{1}{2}}, Z = zRe^{\frac{1}{2}}$

TABLE 1

in the intermediate region, z, $\bar{\eta}$ finite. The corner layer, $z \to 0$, η, ζ finite, shown doubly cross-hatched, is completely three-dimensional in character. Asymptotic methods can be used to join the different regions (Rubin 1966).

It is the three-dimensional corner-layer region that will be considered here. The governing equations for this region will be shown to reduce to four nonlinear, Poisson-like elliptic partial differential equations plus one algebraic relation. Since numerical methods will be required to obtain the final solution, finite boundaries (e.g. $\zeta = Z_0 = 10$) must be specified for the corner region in order that computational times are acceptable. Therefore, the proper far-field boundary conditions are determined by considering analytically the asymptotic behaviour of the corner-layer equations for large η and ζ. In this regard, the symmetry inherent in the geometry plays an important role.

The appearance of an arbitrary constant in the asymptotic formulation requires that an iteration scheme be employed in order to solve uniquely the system of equations. An optimum value of the constant χ is determined by minimizing the effects of mass source terms artificially introduced into the analysis.

2. Derivation of equations

Preliminary analysis

In order to distinguish between the different regions, shown in figure 1, the following convention (given by Rubin 1966) is prescribed. Potential-flow variables are denoted by upper-case letters, boundary-layer quantities by barred lower-case letters, and corner-layer properties by asterisks.

The complete non-dimensionalized governing equations for an arbitrary region are given below. The flow properties have been non-dimensionalized in the following manner: the velocity components with respect to U_∞, the density, temperature and viscosity with their respective free-stream values ρ_∞, T_∞, μ_∞, all lengths with respect to (L) some characteristic dimension, enthalpy with respect to U_∞^2 and pressure with twice the dynamic pressure $\frac{1}{2}\rho_\infty U_\infty^2$.

Continuity:
$$(\rho u)_x + (\rho v)_y + (\rho w)_z = 0; \tag{2.1a}$$

x momentum:
$$\rho(uu_x + vu_y + wu_z) = -p_x + (1/Re)\{[2\mu u_x - \tfrac{2}{3}\mu\Delta]_x + [\mu(u_y + v_x)]_y + [\mu(u_z + w_x)]_z\}; \tag{2.1b}$$

y momentum:
$$\rho(uv_x + vv_y + wv_z) = -p_y + (1/Re)\{[2\mu v_y - \tfrac{2}{3}\mu\Delta]_y + [\mu(v_z + w_y)]_z + [\mu(u_y + v_x)]_x\}; \tag{2.1c}$$

z momentum:

$$\rho(uw_x+vw_y+ww_z) = -p_z+(1/Re)\{[2\mu w_z-\tfrac{2}{3}\mu\Delta]_z+[\mu(w_x+u_z)]_x+[\mu(v_z+w_y)]_y\}; \tag{2.1d}$$

energy:

$$\begin{aligned}&\rho(uh_x+vh_y+wh_z)\\&\quad=(up_x+vp_y+wp_z)+(1/Re)\{(\mu h_x/\sigma)_x+(\mu h_y/\sigma)_y+(\mu h_z/\sigma)_z\\&\qquad+2\mu[u_x^2+v_y^2+w_z^2+\tfrac{1}{2}(u_y+v_x)^2+\tfrac{1}{2}(v_z+w_y)^2+\tfrac{1}{2}(u_z+w_x)^2]-\tfrac{2}{3}\mu\Delta^2\};\end{aligned} \tag{2.1e}$$

equation of state:

$$p = \frac{\gamma-1}{\gamma}\rho h. \tag{2.1f}$$

Subscripts denote partial differentiation and

$$\Delta = u_x+v_y+w_z,$$

$Re = \rho_\infty U_\infty L/\mu_\infty$ is the Reynolds number, and $\sigma = \mu c_p/k$ is the Prandtl number. c_p, c_v and γ are assumed constant. The enthalpy and static temperature are related by $h = T/(\gamma-1)M_\infty^2$, where $M_\infty = U_\infty/(\gamma RT_\infty)^{\frac{1}{2}}$ is the Mach number. It is further assumed that the coefficient of viscosity is proportional to the temperature and that the Prandtl number is equal to unity, i.e.

$$\mu = T, \quad \sigma = 1. \tag{2.2}$$

The wall temperature is constant throughout.

As in the analysis of Rubin (1966), the following series expansions are assumed.

(i) Potential flow:

$$\pi(x,y,z) = \sum_{n=0}^{M} Re^{-\frac{1}{2}n}\,\Pi_n(x,y,z). \tag{2.3}$$

(ii) Boundary layer:

(*a*) $x > 0, y > 0, z > 0$ (region II, figure 1)

$$\pi(x,y,z) = \sum_{n=0}^{M} Re^{-\frac{1}{2}n}\,\bar{\pi}_n(x,Y,z); \tag{2.4a}$$

(*b*) $x > 0$, $y > 0$, $z > 0$ (region III, figure 1)

$$\pi(x,y,z) = \sum_{n=0}^{M} Re^{-\frac{1}{2}n}\,\bar{\pi}_n(x,y,Z). \tag{2.4b}$$

(iii) Corner layer:

$$\pi(x,y,z) = \sum_{n=0}^{M} Re^{-\frac{1}{2}n}\,\pi_n^*(x,Y,Z). \tag{2.5}$$

Here π is any flow property, e.g. $u, v, w, p, h, \ldots$. The zeroth-order potential flow is a uniform stream, so that $U_0 = 1$, $V_0 = W_0 = 0$, etc.

Boundary-layer equations

The equations governing the first-order boundary layer are obtained by putting the series (2.4) into the general Navier–Stokes equations (2.1) and retaining

first-order terms in $Re^{-\frac{1}{2}}$ only, so that the additional no-slip condition neglected in the potential flow is satisfied.

For the boundary layer in region II (cf. figure 1), the familiar two-dimensional equations modified by the inclusion of a cross-flow (w_1) momentum equation are obtained to first order:

$$(\bar{\rho}_0\bar{u}_0)_x+(\bar{\rho}_0\bar{v}_1)_Y = 0, \tag{2.6a}$$

$$\bar{\rho}_0(\bar{u}_0\bar{u}_{0x}+\bar{v}_1\bar{u}_{0Y})+\bar{p}_{0x} = (\bar{\mu}_0\bar{u}_{0Y})_Y, \tag{2.6b}$$

$$\bar{p}_{0Y} = 0, \tag{2.6c}$$

$$\bar{\rho}_0(\bar{u}_0\bar{h}_{0x}+\bar{v}_1\bar{h}_{0Y})-\bar{u}_0\bar{p}_{0x} = \left(\frac{\bar{\mu}_0}{\sigma}\bar{h}_{0Y}\right)_Y+\bar{\mu}_0(\bar{u}_{0Y})^2, \tag{2.6d}$$

$$\bar{p}_0 = \frac{\gamma-1}{\gamma}\bar{\rho}_0\bar{h}_0, \tag{2.6e}$$

$$\bar{\rho}_0(\bar{u}_0\bar{w}_{1x}+\bar{v}_1\bar{w}_{1Y})+\bar{p}_{1z} = (\bar{\mu}_0\bar{w}_{1Y})_Y. \tag{2.6f}$$

The appropriate boundary conditions are at the surface $Y = 0$: $\bar{u}_0 = \bar{v}_1 = \bar{w}_1 = 0$ and $\bar{h}_0 = T_w/[(\gamma-1)M_\infty^2]$; asymptotically as $Y\to\infty$, $\bar{u}_0\to\frac{1}{2}, \bar{h}_0\to 1/[(\gamma-1)M_\infty^2]$ and w_1 asymptotes to a potential value to be determined.

The energy equation may be integrated, consistent with assumptions (2.2), to yield a well-known Crocco integral. Imposing the boundary conditions, the following relationship for temperature is obtained:

$$\bar{t}_0 = T_w+\left(1-T_w+\frac{\gamma-1}{2}M_\infty^2\right)\bar{u}_0-\frac{\gamma-1}{2}M_\infty^2\bar{u}_0^2. \tag{2.7}$$

The solutions of the streamwise momentum equation and the continuity equation can be achieved with the aid of the density transformation of Howarth–Dorodnitsyn (see Stewartson 1964):

$$\bar{u}_0 = f'(\bar{\eta}), \quad v_1 = \frac{1}{(2x)^{\frac{1}{2}}}\left[\bar{t}_0(\bar{\eta}f'-f)-f'\int_0^{\bar{\eta}}\xi\frac{\partial t}{\partial\xi}d\xi\right],$$

where

$$\bar{Y} = \int_0^Y \rho_{2D}\,d\xi \quad \text{and} \quad \bar{\eta} = \bar{Y}/(2x)^{\frac{1}{2}}.$$

The primes denote differentiation with respect to $\bar{\eta}$. The solution exhibits a normal or outflow velocity $\bar{v}_1$, which is absent in the zeroth-order potential flow. The asymptotic value of $\bar{v}_1$ is given by

$$\bar{v}_1\to\beta/(2x)^{\frac{1}{2}} \quad \text{as} \quad \bar{\eta}\to\infty,$$

where

$$\beta = T_w\kappa+\frac{\gamma-1}{2}M_\infty^2 f''(0),$$

$$\kappa = 1{\cdot}21678, \quad f''(0) = 0{\cdot}469600.$$

Analogous results hold for the boundary layer in region III.

Bloom (1966) and Libby (1966), independently, were able to deduce the compressible cross-flow velocity $\bar{w}_1$ (as $z\to 0$ in region II) by solving (2·6*f*) and employing symmetry arguments. Later, in a more complete investigation of the nature of the asymptotic flow field of the incompressible corner layer, Pal & Rubin (1971) determined the entire asymptotic behaviour of the cross-flow

expansion. In the present analysis, the method of Pal & Rubin is extended to include compressibility effects, with Bloom's and Libby's results recovered in a first approximation to the cross-flow velocity.

Corner-layer equations

The equations governing the behaviour of the motion in the corner layer are obtained by substituting (2.5) into (2.1) and retaining only first-order terms. w_1^* and v_1^* are of order $Re^{-\frac{1}{2}}$ and

$$Y = yRe^{\frac{1}{2}}, \quad Z = zRe^{\frac{1}{2}}.$$

The following system is obtained:

$$(\rho_0^* u_{01}^*)_x + (\rho_0^* v_1^*)_Y + (\rho_0^* w_1^*)_Z = 0, \tag{2.8a}$$

$$\rho_0^*(u_0^* u_{0x}^* + v_1^* u_{0Y}^* + w_1^* u_{0Z}^*) + p_{0x}^* = (\mu_0^* u_{0Y}^*)_Y + (\mu_0^* u_{0Z}^*)_Z, \tag{2.8b}$$

$$p_{0Y}^* = 0, \quad p_{1Y}^* = 0, \tag{2.8c}$$

$$\rho_0^*(u_0^* v_{1x}^* + v_1^* v_{1Y}^* + w_1^* v_{1Z}^*) + p_{2Y}^* = (2\mu_0^* v_{1Y}^*)_Y + (\lambda^*[u_{0x}^* + v_{1Y}^* + w_{1Z}^*])_Y + (\mu_0^*[v_{1Z}^* + w_{1Y}^*])_Z + (\mu_0^* u_{0Y}^*)_x, \tag{2.8d}$$

$$p_{0Z}^* = 0, \quad p_{1Z}^* = 0, \tag{2.8e}$$

$$\rho_0^*(u_0^* w_{1x}^* + v_1^* w_{1Y}^* + w_1^* w_{1Z}^*) + p_{2Z}^* = (2\mu_0^* w_{1Z}^*)_Z + (\lambda^*[u_{0x}^* + v_{1Y}^* + w_{1Z}^*])_Z + (\mu_0^*[w_{1Y}^* + v_{1Z}^*])_Y + (\mu_0^* u_{0Z}^*)_x, \tag{2.8f}$$

$$\rho_0^*(u_0^* h_{0x}^* + v_1^* h_{0Y}^* + w_1^* h_{0Z}^*) - (u_0^* p_{0x}^* + v_1^* p_{0Y} + w_1^* p_{0Z}^*) = (\mu_0^* h_{0Y}^*/\sigma)_Y + (\mu_0^* h_{0Z}^*/\sigma)_Z + \mu_0^*([u_{0Y}^*]^2 + [u_{0Z}^*]^2), \tag{2.8g}$$

$$p_0^* = \frac{\gamma - 1}{\gamma} \rho_0^* h_0^* \tag{2.8h}$$

and

$$\lambda^* = -\tfrac{2}{3}\mu_0^*.$$

Note that the pressure p_2^* appearing in the crosswise momentum equations is of second order. For the case under consideration (two intersecting flat plates), p_0^* is constant and equal to its free-stream value.

Combining the energy and streamwise momentum equations, we find

$$\rho_0^*(u_0^* H_{0x}^* + v_1^* H_{0Y}^* + w_1 H_{0Z}^*) = (\mu_0^* H_{0Y}^*)_Y + (\mu_0 H_{0Z}^*)_Z, \tag{2.9}$$

where

$$H_0^* = h_0^* + \tfrac{1}{2} u_0^{*2}.$$

Comparing (2.9) with (2.8*b*) and with $p_{0x}^* = 0$, it is observed that a solution to (2.9) satisfying all the boundary conditions is once again the Crocco integral. In terms of the temperature this becomes

$$t_0^* = T_w + \left(1 - T_w + \frac{\gamma - 1}{2} M_\infty^2\right) u_0^* - \frac{\gamma - 1}{2} M_\infty^2 u_0^{*2}. \tag{2.10}$$

It is important to point out that the Crocco integral is applicable here even for a three-dimensional flow, and is independent of the normal and spanwise velocities. This result greatly simplifies the ensuing analysis. The temperature has now been determined as a function of the streamwise velocity u_0^*, and represents a solution for the energy equation. Furthermore, from the equation of

state, and with the model-fluid assumptions, the density and viscosity relationships become

$$\mu_0^* = t_0^* = C, \quad \rho_0^* = 1/t_0^* = 1/C. \tag{2.11a,b}$$

In order to simplify further the subsequent calculations, similarity variables are defined:

$$u = u_0^*, \quad v = v_1^*(2x)^{\frac{1}{2}}, \quad w = w_1^*(2x)^{\frac{1}{2}},$$

$$p = p_2^* 2x, \quad \rho = \rho_0^*, \quad \mu = \mu_0^*,$$

and

$$\eta = Y/(2x)^{\frac{1}{2}}, \quad \zeta = Z/(2x)^{\frac{1}{2}}.$$

In addition it is also convenient here to introduce the new variables (see Rubin & Grossman 1971)

$$\phi = \eta u - v, \tag{2.12a}$$

$$\psi = \zeta u - w, \tag{2.12b}$$

$$\theta = \psi_\eta - \phi_\zeta, \tag{2.12c}$$

$$\Lambda = \phi_\eta + \psi_\zeta. \tag{2.12d}$$

The second-order pressure p_2^* appearing in (2.8f) and (2.8g) can be eliminated by cross differentiation of the two equations. In addition, derivatives of ρ and μ are replaced by derivatives of C with respect to u. Thus, μ_η becomes $\partial C/\partial u\, u_\eta$, and

$$\frac{\partial C}{\partial u} = C_u = \left(1 - T_w + \frac{\gamma - 1}{2} M_\infty^2\right) - (\gamma - 1) M_\infty^2 u,$$

$$\frac{\partial^2 C}{\partial u^2} = C_{uu} = -(\gamma - 1) M_\infty^2.$$

In the incompressible limit

$$C = 1, \quad C_u = C_{uu} = 0.$$

With these definitions, the following set of equations results:

$$C^2 \nabla^2 u + \phi u_\eta + \psi u_\zeta = -C C_u (u_\eta^2 + u_\zeta^2), \tag{2.13a}$$

$$\begin{aligned} &C^3 \nabla^2 \theta + C[\phi\theta_\eta + \psi\theta_\zeta + 2u(\theta + \eta u_\zeta - \zeta u_\eta)] \\ &= C_u(u_\eta[\phi\phi_\zeta + \psi\psi_\zeta - \zeta u^2 - 2C^2(\Lambda_\zeta + \theta_\eta)] - u_\zeta[\psi\psi_\eta + \phi\phi_\eta - \eta u^2 - 2C^2(\Lambda_\eta - \theta_\zeta)]) \\ &\quad + \left(\frac{(\psi^2 - \phi^2)(\psi_\eta + \phi_\zeta) + 2\phi\psi(\phi_\eta - \psi_\zeta)}{(\phi^2 + \psi^2)}\right)((u_\zeta^2 + u_\eta^2)(CC_u^2 - C^2 C_{uu}) \\ &\quad + (C_u(\phi u_\eta + \psi u_\zeta))) + \frac{2C^2}{\phi^2 + \psi^2}([\psi(\phi_\eta - \psi_\zeta) - \phi(\psi_\eta + \phi_\zeta)][C_u(u_\eta\{\psi_\zeta - 2u\} - \psi_\eta u_\zeta) \\ &\quad + C(\Lambda - 2u)_\eta] + [\phi(\phi_\eta - \psi_\zeta) + \psi(\psi_\eta + \phi_\eta)][C_u(u_\zeta\{\phi_\eta - 2u\} - \phi_\zeta u_\eta) \\ &\quad + C(\Lambda - 2u)_\zeta]), \end{aligned} \tag{2.13b}$$

$$C(\Lambda - 2u) = C_u(\phi u_\eta + \psi u_\zeta). \tag{2.13c}$$

In order that numerical techniques may be applied to the corner-layer equations, the continuity and vorticity relations (2.12c,d) are cross-differentiated, to yield

$$\nabla^2 \phi = \Lambda_\eta - \theta_\zeta, \quad \nabla^2 \psi = \theta_\eta + \Lambda_\zeta. \tag{2.13d,e}$$

These equations admit mass and vorticity sources, in the sense that unknown harmonic junctions $V(\eta, \zeta)$ and $M(\eta, \zeta)$ can be added to (2.12*c*, *d*), respectively, without changing (2.13*d*) or (2.13*e*). These source terms must be eliminated in the final solution. Further discussion of this matter will be presented later.

Equations (2.13) and (2.14) constitute the set of five governing equations, consisting of four nonlinear elliptic Poisson-like partial differential equations and one algebraic equation. For their solution, conditions must be specified on all boundaries with asymptotic matching of the potential and boundary-layer regions. These relations will be discussed in § 3.

The theory developed here is not restricted to a geometry with a sharp right-angle intersection. A fillet is permissible at the corner intersection as long as its radius of curvature is small compared with the corner-layer thickness. Consideration of this geometry is given by Weinberg (1972). Significantly, the influence of the fillet is confined to a region of the order of the fillet radius. This indicates that the general flow behaviour will not be appreciably influenced by modifications near the corner point.

3. Asymptotic analysis and boundary conditions

In § 3 the appropriate boundary conditions for the corner layer are developed. Since the governing equations are elliptic in nature (as previously discussed), conditions must be specified at all boundaries. In addition to the usual conditions specified at the wall surfaces, asymptotic results are determined in order to match the corner-layer to the boundary-layer motions that exist along each of the two intersecting walls, and to an irrotational inviscid stream. This asymptotic analysis allows for a finite computational domain, and reduces computer storage and calculation times. Furthermore, the inherent symmetry along the angle bisector $\eta = \zeta$ allows for a further simplification, as only one of the resulting triangular regions need be treated (cf. figure 2).

In this discussion the lower triangular region bounded by

$$\eta = 0, \quad 0 \leqslant \zeta \leqslant Z_0,$$
$$\eta = \zeta, \quad 0 \leqslant \zeta \leqslant Z_0,$$
$$\zeta = Z_0, \quad 0 \leqslant \eta \leqslant Z_0,$$

is considered. The boundary conditions across and on the symmetry line $\eta = \zeta$ are

$$u_\eta = u_\zeta, \quad \Lambda_\eta = \Lambda_\zeta, \quad \phi_\eta = \psi_\zeta, \quad \phi = \psi, \quad \theta = 0. \tag{3.1}$$

On $\eta = 0$, for all ζ, we specify

$$u = \phi = \psi = \Lambda = 0, \quad \theta = \psi_\eta, \quad t = T_w. \tag{3.2a–c}$$

Finally, u, ϕ, ψ, Λ and θ must asymptote to the boundary-layer flow as $\zeta \to \infty$, $\eta/\zeta \to 0$ and potential flow for $\zeta \to \infty$, $\eta \leqslant \zeta$. The analysis of Pal & Rubin (1971) for the incompressible case has shown that the corner-layer variables decay algebraically into the outer layers, and hence, several terms in the asymptotic series are necessary to describe adequately the flow behaviour at a finite boundary $\zeta = Z_0$.

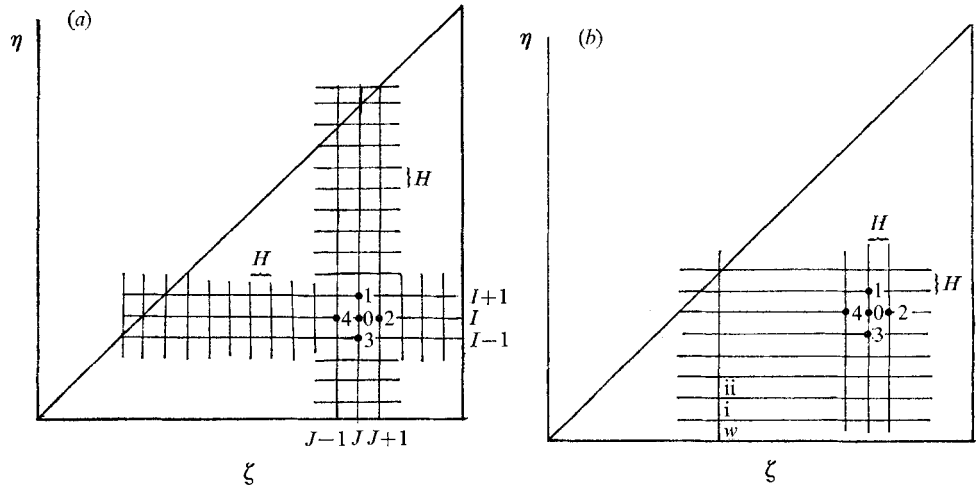

FIGURE 2. Finite-difference grid: (*a*) explicit, (*b*) implicit.

Corner-layer/boundary-layer matching

The object of the following discussion is to find formal asymptotic expansions

$$u(\eta,\zeta) \sim \sum_{n=0}^{\infty} u_n(\bar{\eta},\lambda)\,\zeta^{-n}, \tag{3.3a}$$

$$\phi(\eta,\zeta) \sim \sum_{n=0}^{\infty} \phi_n(\bar{\eta},\lambda)\,\zeta^{-n}, \tag{3.3b}$$

$$\psi(\eta,\zeta) \sim \sum_{n=0}^{\infty} \psi_n(\bar{\eta},\lambda)\,\zeta^{-n+1}, \tag{3.3c}$$

$$\theta(\eta,\zeta) \sim \sum_{n=0}^{\infty} \theta_n(\bar{\eta},\theta)\,\zeta^{-n+1}, \tag{3.3d}$$

$$\Lambda(\eta,\zeta) \sim \sum_{n=0}^{\infty} \Lambda_n(\bar{\eta},\Lambda)\,\zeta^{-n}, \tag{3.3e}$$

valid for large values of ζ and arbitrary $\eta \leqslant \zeta$, where

$$\lambda = \ln\zeta, \quad \bar{\eta} = \int_0^{\eta} \rho_{2D}\,d\eta,$$

and $$\rho_{2D} = \frac{1}{C_0(\bar{\eta})} = \left\{T_w + \left(1 - T_w + \frac{\gamma-1}{2}M_\infty^2\right)f'(\bar{\eta}) - \frac{\gamma-1}{2}M_\infty^2 f'^2(\bar{\eta})\right\}^{-1}.$$

Note that the density appearing under the integral sign is the two-dimensional value. Since the two-dimensional boundary-layer solution is known in terms of $\bar{\eta}$, it is employed here to facilitate matching.† Derivatives with respect to η are given by

$$\frac{\partial}{\partial\eta} = \frac{1}{C_0(\bar{\eta})}\frac{\partial}{\partial\bar{\eta}},$$

† A three-dimensional density transformation analogous to that of Howarth–Dorodnitsyn for the two-dimensional case does not exist, to the author's knowledge. If such a transformation did exist, then any compressible corner-flow solution could be obtained by transforming it into incompressible form.

while η and $\bar{\eta}$ are related by

$$\eta = T_w\bar{\eta} + \left(1 - T_w + \frac{\gamma-1}{2}M_\infty^2\right)f(\eta) - \frac{\gamma-1}{2}M_\infty^2(f''(\bar{\eta}) - f(\bar{\eta})f'(\bar{\eta})) + \frac{\gamma-1}{2}M_\infty^2 f''(0).$$

The coefficients $u_n, \theta_n, \phi_n, \psi_n$ and Λ_n are assumed to depend on $\bar{\eta}$ and also on ζ, in that we assume a polynomial dependence on $\lambda = \ln\zeta$. (See Pal & Rubin 1971 for further details.) The first few terms of the asymptotic series do not depend on λ, since the governing equations and boundary conditions can be satisfied with the omission of the $\partial/\partial\lambda$ terms. Since only the first 3 terms, $n = 0, 1, 2$, will be considered here, the resulting equations will be independent of λ. Substituting the asymptotic series (3.3) into the governing equations (2.13, 2.14), we obtain recursive relations for the flow variables. (See Weinberg 1972 for a discussion of the generalized expansions.)

The solutions of the equations for $n = 0, 1, 2,$ will now be discussed.

Zeroth-order solution. For $n = 0$, the following equations are obtained:

$$\theta_0 = \frac{1}{c_0}\psi_0', \tag{3.4a}$$

$$\Lambda_0 = \frac{1}{C_0}\phi_0' + \psi_0, \tag{3.4b}$$

$$\phi_0' + C_0(\psi_0 - 2u_0) - \frac{C_{u0}}{C_0}\phi_0 u_0' = 0, \tag{3.4c}$$

$$u_0' + \phi_0\frac{u_0'}{C_0} = 0, \tag{3.4d}$$

$$C_0\left(\frac{\phi_0}{C_0}\theta_0' + \psi_0\theta_0 + 2u_0\theta_0 - \frac{2u_0}{C_0}u_0'\right) + C_0\left(\theta_0'' - \frac{C_{u0}}{C_0}u_0'\theta_0'\right)$$
$$= \frac{C_{u0}}{C_0}u_0'(\psi_0^2 - u_0^2) - 2C_{u0}u_0'\theta_0' + \theta_0\left(\frac{(C_0C_{u0}^2 - C_{uu}C_0^2)}{C_0}u_0'u_0' + C_{u0}\Gamma_0\right), \tag{3.4e}$$

where $$\theta_0 = \psi_{0\eta} + \phi_{0\zeta}, \quad \Gamma_0 = \phi_0 u_{0\eta} + \psi_0 u_{0\zeta}.$$

The boundary conditions are, at the surface $\bar{\eta} = 0$,

$$u_0 = \phi_0 = \psi_0 = \Lambda_0 = 0,$$

while, for $\bar{\eta} \to \infty$,

$$u_0 = 1 + o(\bar{\eta}^{-N}), \quad \theta_0 = o(\bar{\eta}^{-N}) \quad \text{for} \quad N > 0.$$

Comparing (3.4*d*) with the Blasius equation

$$f''' + ff'' = 0,$$

it is observed that a solution of (3.4*d*), satisfying all boundary conditions, is

$$u_0 = f' \quad \phi_0 = C_0 f. \tag{3.5a,b}$$

Solving (3.4*a–c*) for the remaining unknowns, we obtain

$$\psi_0 = f', \quad \theta_0 = f''/C_0, \quad \Lambda_0 = 2f' + \frac{C_{u0}}{C_0}ff''. \tag{3.5c–e}$$

These functions satisfy all the boundary conditions and (3.4*e*) identically.

First-order solution. Retaining terms of $O(\zeta^{-1})$ in the asymptotic equations, we obtain

$$\left(\frac{\phi_1 - C_{u0} f u_1}{C_0}\right)' + 2\left(\frac{C_{u0}}{C_0} f' - 1\right) u_1 = 0, \tag{3.6a}$$

$$u_1'' + \left(\frac{C_{u0}}{C_0} f'' + f\right) u_1' + \left(-\frac{C_{u0}}{C_0} f f'' + \frac{C_{uu}}{C_0} f''^2 - \frac{C_{u0}^2}{C_0^2} f''^2 - f'\right) u_1 + f''\left(\frac{\phi_1 - C_{u0} f u_1}{C_0}\right) = 0, \tag{3.6b}$$

$$\Lambda_1 = \phi_1'/C_0, \quad \theta_1 = \psi_1'/C_0. \tag{3.6c,d}$$

The boundary conditions are, at the surface $\bar{\eta} = 0$,

$$u_1 = \phi_1 = \psi_1 = \Lambda_1 = 0,$$

while, for $\bar{\eta} \to \infty$,

$$u_1 = o(\bar{\eta}^{-N}), \quad \theta_1 = o(\bar{\eta}^{-N}) \quad \text{for} \quad N > 0.$$

Combining (3.6*a*, *b*), ϕ_1 may be eliminated, and a third-order equation in u_1 is obtained:

$$u_1''' + 2f u_1'' + f u_1'^2 + (f'' + f f') u_1 + g_1'' + f g_1' - 2f' g_1 = 0, \tag{3.7}$$

where

$$g_1 = \frac{C_{u0}}{C_0} f'' u_1.$$

Defining

$$U_1 = u_1' + f u_1 + g_1,$$

(3.7) may be transformed to

$$U_1'' + f U_1' - 2f' U_1 = 0. \tag{3.8}$$

The only solution of this equation is

$$U_1 \equiv 0, \quad \phi_1 = u_1 \equiv 0. \tag{3.9}$$

It is significant that the part of (3.7) involving u_1 terms alone is identical with the incompressible equation derived by Pal & Rubin (1971). Thus, (3.8) is obtained independent of the compressibility. Therefore, any statement concerning the incompressible-flow case should be just as valid for the compressible flow. Libby & Fox (1963) have proved that eigenvalues of (3.8) do not exist. In a similar manner, it can be shown (Weinberg 1972) that

$$\psi_1(\bar{\eta}) = -\beta f'' \int_0^{\bar{\eta}} \frac{1}{f''}\left[\int_0^{\tau} C_0(\omega)\, d\omega - \beta\right] d\tau \equiv -\beta g_c(\bar{\eta}), \tag{3.10}$$

where

$$\beta = T_w \kappa + \frac{\gamma - 1}{2} M_\infty^2 f''(0), \tag{3.11}$$

and

$$\kappa = \lim_{\eta \to \infty} (\bar{\eta} f' - f) = 1{\cdot}21678.$$

The function $g_c(\bar{\eta})$ is identical with the Libby solution for the cross-flow velocity w in the boundary layer, and is strictly valid only at $\zeta = \infty$. Figures 3(*a*, *b*) show the variation of $g_c(\bar{\eta})$ with respect to wall temperature and Mach number. The representations for w given by $g_c(\nu)$ and by (3.17*b*), for finite ζ, are compared.

Finally, from (3.6*c*, *d*), we obtain

$$\Lambda_1 = 0, \quad \theta_1 = \frac{-\beta}{C_0} g_c'(\bar{\eta}). \tag{3.12}$$

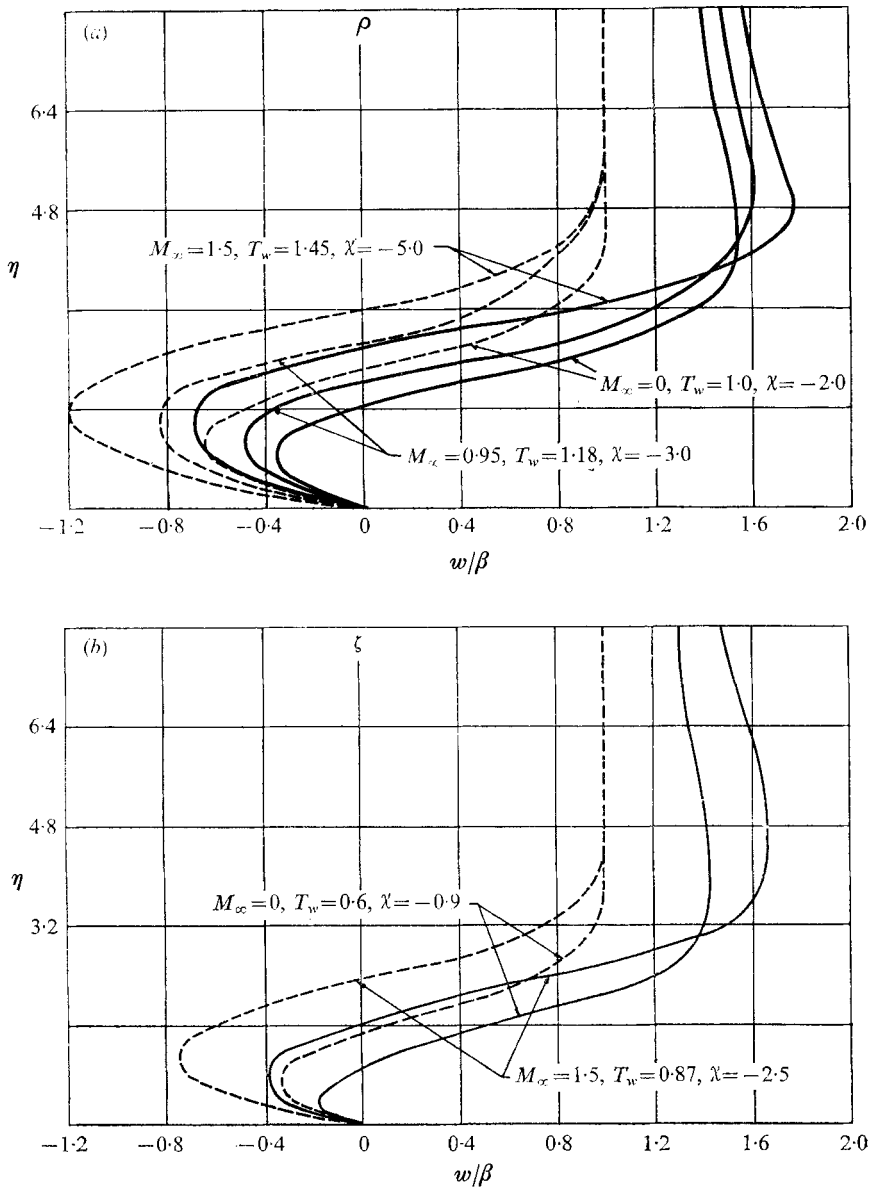

FIGURE 3. Asymptotic cross-flow profiles: (*a*) adiabatic, (*b*) cold wall ($T_w/T_{stag} = 0{\cdot}6$). ----, Libby (1966); ———, (3.17*b*) at $Z_0 = 9.60$.

The second-order ($n = 2$) equations can be obtained in a like fashion (Weinberg 1972), and the solutions are

$$u_2 = \frac{f''}{C_0}\eta, \tag{3.13a}$$

$$\phi_2 = C_0 f + \eta\left\{3f' + \frac{C_{u0}}{C_0}ff''\right\}, \tag{3.13b}$$

$$\psi_2 = \eta \frac{f''}{C_0} + 4f', \tag{3.13c}$$

$$\theta_2 = \frac{5f''}{C_0} - \eta \left\{ \frac{ff''}{C_0^2} + \frac{C_{u0}}{C_0^3} f''^2 \right\}, \tag{3.13d}$$

$$\Lambda_2 = 2\frac{C_{u0}}{C_0} ff'' + \frac{f''}{C_0} \left\{ 2 + \frac{C_{uu}}{C_0} ff'' - \frac{C_{u0}^2}{C_0^2} ff'' + \frac{C_{u0}}{C_0} f' - \frac{C_{u0}}{C_0} f^2 \right\} \eta. \tag{3.13e}$$

In Rubin & Grossman (1971) it is shown that at $n = 1$ an arbitrary constant enters into the asymptotic series. The significance of this will be discussed shortly. With (3.5), (3.9), (3.10), (3.12) and (3.13) we now have three terms in the asymptotic expansion for large ζ and $\eta/\zeta \to 0$.

Corner-layer/potential-flow matching

For $\min(\eta, \zeta) \to \infty$, it must also be possible to match the corner layer to an outer irrotational flow. In order that the leading vorticity components vanish with exponential speed, we find that

$$u = 1 + o(\eta^{-N}) \quad (N > 0); \tag{3.14a}$$

and, from the Crocco integral, the temperature is a function of u only, so that

$$T = 1 + o(\eta^{-N}) \quad (N > 0). \tag{3.14b}$$

From the streamwise vorticity component,

$$v_\eta - w_\zeta = o(\eta^{-N}) \quad (N > 0). \tag{3.14c}$$

These relations imply that

$$\theta = o(\eta^{-N}) \quad (N > 0), \tag{3.14d}$$

$$\Lambda = 2 + o(\eta^{-N}) \quad (N > 0). \tag{3.14e}$$

It may be further shown, from the definition (2.12c) of θ, that

$$w_\eta - v_\zeta = o(\eta^{-N}) \quad (N > 0). \tag{3.14f}$$

With the model-fluid assumption and (3.14b), the density also exhibits exponential decay into the potential flow. Therefore, the following formulation will be independent of any explicit compressibility effects. We therefore seek conjugate harmonic functions for v and w, satisfying (3.14c,f) and possessing the proper algebraic decay, as well as fulfilling all the required symmetric conditions. From the analysis of Pal & Rubin (1971), the following solutions for ϕ and ψ are obtained:

$$(\phi - i\psi)\exp\{\tfrac{1}{4}i\pi\} = (\eta - i\zeta)\exp\{\tfrac{1}{4}i\pi\} - (2\beta)^{\frac{1}{2}} + 4\chi\tau^{-1} - (2\beta)^{\frac{1}{2}}\tau^{-2} + O(\tau^{-3}), \tag{3.15}$$

where $\tau = (\eta + i\zeta)\exp\{-\frac{1}{4}i\pi\}$, χ is a real constant to be determined, and β has previously been defined by (3.11). Note that compressibility effects enter into (3.15) through the parameter β, which is a function of Mach number and wall temperature.

$\eta = 0$	$\eta = \zeta$	$\zeta = Z_0$
$M_\eta = 0$	$M_\eta - M_\zeta = 0$	$M = 0$
$V = 0$	$V = 0$	$V = 0$

TABLE 2

Therefore, the asymptotic boundary conditions for $\zeta \to \infty$ and all η become

$$u = f' + \chi\left\{\frac{f''}{C_0}\eta\right\}\zeta^{-2}, \tag{3.16a}$$

$$\phi = C_0 f + \chi\left\{\left[C_0 f + \left(3f' + \frac{C_{u0}}{C_0}ff''\right)\eta - 4\eta + \beta\right]\zeta^{-2} + \frac{4\eta}{\eta^2+\zeta^2} + \frac{\beta}{(\eta^2+\zeta^2)^2}(\eta^2 + 2\eta\zeta - \zeta^2)\right\}, \tag{3.16b}$$

$$\psi = f'\zeta - \beta g_c + \chi\left\{\left[4f' + \frac{f''}{C_0}\eta - 4\right]\zeta^{-1} + \frac{4\zeta}{\eta^2+\zeta^2} + \frac{\beta}{(\eta^2+\zeta^2)^2}(\eta^2 - 2\eta\zeta - \zeta^2)\right\}, \tag{3.16c}$$

$$\theta = \frac{f''}{C_0}\zeta - \frac{\beta}{C_0}g_c' + \chi\left\{\frac{5f''}{C_0} - \frac{f''}{C_0^2}\left(f + \frac{C_{u0}}{C_0}f''\right)\eta\right\}\zeta^{-1}, \tag{3.16d}$$

$$\Lambda = \left[2f' + \frac{C_{u0}}{C_0}ff''\right] + \chi\left\{2\frac{C_{u0}}{C_0}ff'' + \frac{f''}{C_0}\eta\left(2 + \frac{C_{uu}}{C_0}ff'' - \frac{C_{u0}^2}{C_0}ff'' + \frac{C_{u0}}{C_0}f' - \frac{C_{u0}}{C_0}f^2\right)\right\}\zeta^{-2}. \tag{3.16e}$$

The secondary velocities v and w can now be obtained from the series (3.16) and definition (2.12):

$$v = \eta f'(\bar{\eta}) - C_0(\bar{\eta})f(\bar{\eta}) + \chi\left\{C_0(\bar{\eta})f(\bar{\eta}) - \frac{f''(\bar{\eta})}{C_0(\bar{\eta})}\eta^2 + \eta\left(3f'(\bar{\eta}) + \frac{C_{u0}}{C_0}f(\bar{\eta})f''(\bar{\eta}) - 4\eta + \beta\right)\right\}\zeta^{-2} + \frac{4\chi\eta}{(\eta^2+\zeta^2)} + \frac{\beta\chi}{(\eta^2+\zeta^2)}[\eta^2 + 2\eta\zeta - \zeta^2], \tag{3.17a}$$

$$w = \beta g_c(\bar{\eta}) - 4\chi\left[f'(\bar{\eta}) - 1 + \frac{\zeta^2}{\eta^2+\zeta^2}\right]\zeta^{-1}. \tag{3.17b}$$

With boundary conditions (3.1), (3.2) and (3.16), and the system (2.13), the problem is completely specified. As in the incompressible case, the final system (2.13) includes the differentiated forms of (2.12*c*, *d*). However, if harmonic mass and vorticity source terms $V(\eta, \zeta)$ and $M(\eta, \zeta)$ appear on the right-hand sides of (2.12*c*, *d*), respectively, the final equations (2.13) would remain unchanged. We therefore seek solutions for which M and V vanish everywhere. The boundary conditions (3.1), (3.2) and (3.16) ensure the boundary values for M and V shown in table 2.

When the error in χ is a minimum $|M|$ and $|V|$ attain their minimum values, (2.12*c*, *d*) will be satisfied to the accuracy of the finite-difference scheme and the maximum accuracy allowed by series (3.16).

Method	H	Z_0	No. of iterations	Time (s)
ADI	0·40	9·60	80	40
ADI	0·20	9·80	30	60
GS	0·40	9·60	600	60

TABLE 3

4. Numerical analysis

Two finite-difference equations are employed in the numerical solution of the set of governing equations (2.13). These iterative techniques are conveniently categorized as either explicit or implicit, depending on whether a pivotal point is expressed in terms of other known or unknown values, respectively.

Explicit methods are, in general, simple to program. However, they are limited by somewhat severe stability criteria, so that the grid spacing cannot be chosen arbitrarily. For instance, the incompressible-flow calculation of Rubin & Grossman (1971) indicated that the step sizes were limited by the size of the domain (i.e. the choice of Z_0).

The Gauss–Seidel method was adopted here for the initial calculations. Past success with this method for incompressible flow and the ease of computer coding outweighed any disadvantages associated with stability problems or slow convergence rates. A detailed discussion of this approach for the incompressible calculations can be found in Rubin & Grossman (1971). Solutions for a variety of stream conditions for both cold and adiabatic walls have been obtained. In many cases the convergence was quite slow or instabilities were encountered (Weinberg 1972). These results led the authors to consider a second numerical method both as a check on the converged Gauss–Seidel calculations, and in order to obtain more rapid solutions for wider range of flow conditions. The alternating-direction implicit (ADI) method of Peaceman & Rachford (1955) was chosen.

The finite-difference approximations to the corner-layer equations and their implementation are presented in detail by Weinberg (1972), where the two schemes are compared with regard to convergence rate, stability and ease of computer coding. Only a brief review is given here. It was shown that the ADI and Gauss–Seidel techniques converge at approximately the same rate when the acceleration parameter of the ADI method is unity. For values of this parameter less than unity, convergence improved, but the calculations were sometimes unstable. For values greater than 1·0 the convergence rate was poor. It should be noted that the diagonal boundary and explicit treatment of the vorticity boundary conditions could account for the poor performance of the ADI method. For cases where stability was not a problem, the Gauss–Seidel method was preferred. In several instances where the Gauss–Seidel calculations were unstable, ADI results were obtained. Typical computer running times are given in table 3.

The error associated with any of the converged solutions is a function of the error inherent in the finite-difference approximation, the truncation error at the boundary in series (3.16), and any inaccuracy associated with the constant χ. The effect of these errors on the solutions is now briefly discussed.

It can be shown (Weinberg 1972) that retaining terms in the asymptotic series up to $O(\zeta^{-2})$ for u and ϕ, and up to $O(\zeta^{-1})$ for ψ and θ, would be acceptable in obtaining solutions of approximately 10% accuracy. An examination of the asymptotic series for the incompressible-flow case showed that neglecting higher-order terms had but a minor effect on the solutions. The numerical calculations have also established this fact. Calculations for compressible cases indicate that the errors incurred are well within the desired accuracy. We can conclude that the truncated asymptotic series applied at $\zeta = 9{\cdot}60$ adequately represents the boundary conditions with the desired accuracy for most of the cases considered. It is observed, however, that by raising the wall temperature and/or Mach number, the asymptotic boundary conditions must be applied at values of ζ greater than those for the incompressible flow. This is due to the increase in boundary-layer thickness. Decreasing the wall temperature has the opposite effect: the viscous zone is thinner and the gradients near the wall increase. An examination of the leading terms in the asymptotic representation of θ_w leads to

$$\theta_w \sim \zeta \frac{f''(0)}{T_w} - \frac{g_c'(0)}{T_w} + O(\zeta^{-1}). \tag{4.1}$$

Therefore, as $T_w \to 0$, $\theta_w \to \infty$, and resolution becomes a severe problem. Finer meshes are required, and this results in longer computing times and increased computer storage. However, for the colder wall, and therefore thinner boundary layers, the asymptotic formulae are applicable at somewhat smaller values of Z_0 than those required for the heated wall cases.

From the above considerations it is apparent that limitations must be placed on the flows that can be investigated by the methods presented herein. Calculations indicate that flows with Mach numbers less than 2·0 and $T_w/T_{\text{stag}} > 0{\cdot}40$ can be considered within the limitations previously specified. At higher Mach numbers, hypersonic interaction effects become important, and must be taken into account. Furthermore, the cold wall cases $T_w/T_{\text{stag}} < 0{\cdot}40$ are generally important only for the higher Mach number flows.

In addition to the series truncation error, which is of $O(Z_0^{-2})$, the finite-difference discretization error is estimated to be $O(H^2)$. With $Z_0 = 9{\cdot}60$ and $H = 0{\cdot}40$, the dominant error results from the choice of step size. Reducing the mesh width to 0·20 should optimize the calculations. Finer grids are necessary to maintain this resolution in extreme cold wall cases. For problems where the discretization error can be estimated as a function of H, a very useful alternative to decreasing the step size is a simple extrapolation due to Richardson (see Smith 1965). This procedure was considered by Rubin & Grossman (1971). For a rectangular corner-layer region, with error of $O(H^2)$, if σ_1 and σ_2 denote solutions for H_1 and H_2, respectively, with $H_1 = 2H_2$ an improved solution $\overline{\sigma}$ is given by

$$\overline{\sigma} = \tfrac{1}{3}(4\sigma_2 - \sigma_1).$$

The error is then estimated to be $O(H_2^4)$. All final solutions have been obtained with this extrapolation procedure.

Finally, in the asymptotic analysis (§3) the appearance of an arbitrary constant χ was discussed. The value of χ is specified when the harmonic functions V

M_∞	T_w	$\frac{T_w}{T_{stag}}$	χ	$\lvert M\rvert_{max}$	$\lvert V\rvert_{max}$
0·00	0·60	0·60	−0·9	0·04	0·03
0·50	1·05	1·00	−2·50	0·02	0·05
0·95	1·18	1·00	−3·00	0·02	0·03
1·50	1·45	1·00	−5·00	0·06	0·15
1·50	0·87	0·60	−2·50	0·02	0·05
2·00	1·08	0·60	−4·50	0·04	0·13
2·00	0·70	0·40	−1·50	0·07	0·10

TABLE 4

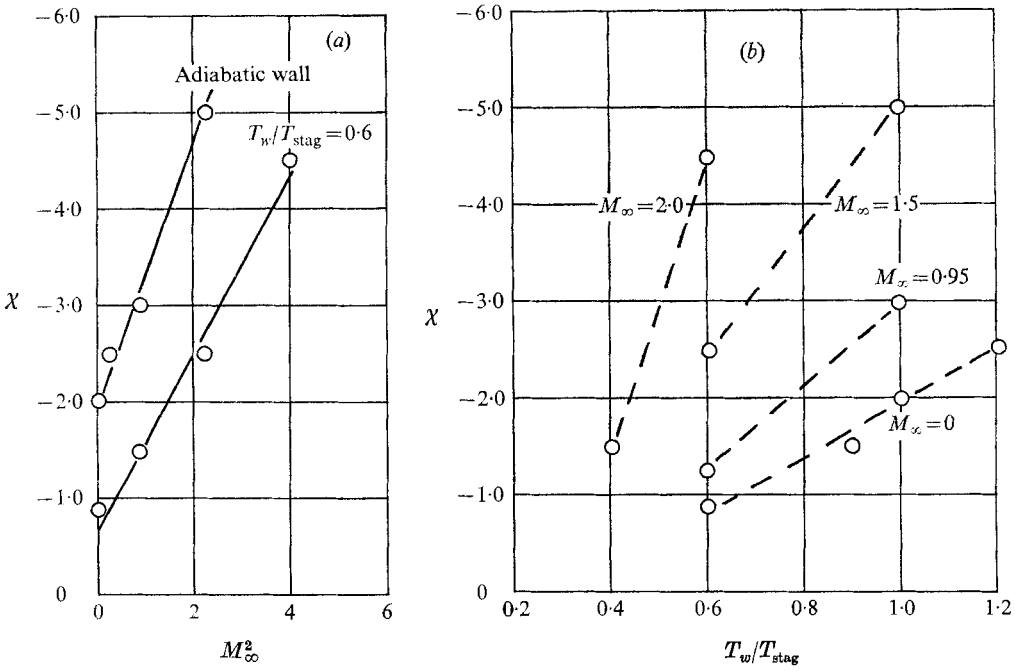

FIGURE 4. Compressibility effects on χ: (*a*) adiabatic (*b*) cold wall ($T_w/T_{stag} = 0·6$).

and M introduced into (2.12*c*, *d*) are filtered out. This is achieved by an iterative procedure identical with that presented by Rubin & Grossman (1971) for incompressible flow, and discussed in greater detail for compressible flow by Weinberg (1972). The optimum value of χ associated with the minimum absolute values of M and V is generally found to occur when the integrated average value of M over the entire grid approaches zero (i.e. positive and negative contributions cancel). Table 4 presents representative compressible-flow conditions with the associated values of χ and $|V|_{max}$ and $|M|_{max}$.

The variation of χ with Mach number and wall temperature has been determined and is presented in figure 4. For a given ratio of wall temperature to stagnation temperature, χ increases linearly with M_∞^2. A linear variation of χ with respect to T_w/T_{stag} is also predicted, for fixed free-stream Mach number.

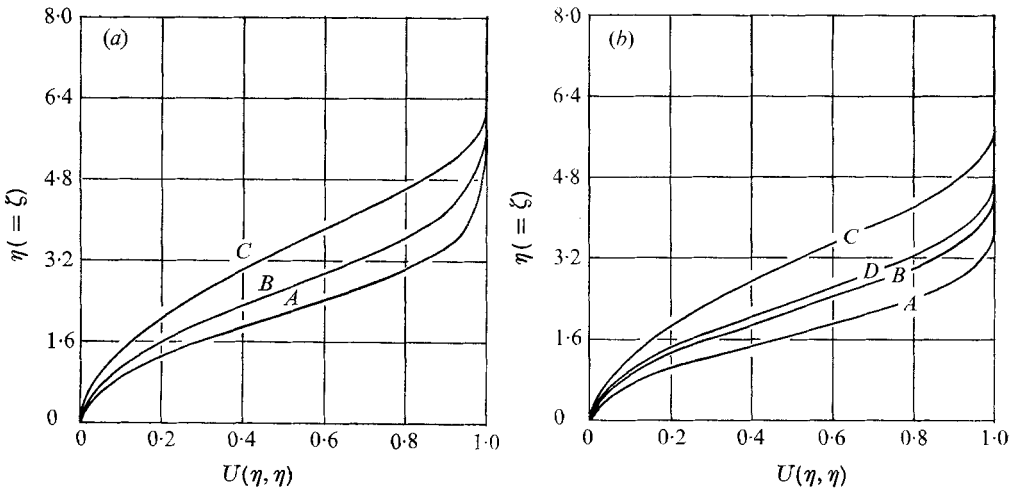

FIGURE 5. Streamwise velocity along symmetry line: (*a*) adiabatic, (*b*) cold wall ($T_w/T_{stag} = 0{\cdot}6$).

		A	*B*	*C*		*A*	*B*	*C*	*D*
M_∞		0	0·95	1·50		0	0	2·0	1·5
T_w	(*a*)	1·0	1·18	1·45	(*b*)	0·6	1·0	1·08	0·87
χ		−2·5	−3·0	−5·0		−0·9	−2·5	−4·5	−2·5

5. Discussion of numerical results

The numerical solutions obtained for the compressible flows considered here are all in very good agreement with the predicted asymptotic behaviour determined in § 3. The algebraic decay of the flow variables into the boundary layer $\zeta \to \infty$, $\eta/\zeta \to 0$ has been obtained numerically. In addition, the solutions show that the normal velocity v approaches its asymptotic boundary-layer value somewhat more rapidly than the cross-flow velocity w. This is in agreement with the predicted asymptotic decay.

Figures 5 and 6 present the streamwise and secondary-flow velocities along the diagonal. Typical adiabatic and cold wall ($T_w/T_{stag} = 0{\cdot}6$) cases are compared. Several interesting features are noted. The streamwise velocity exhibits a much more rapid decay into the outer potential flow, $\eta, \zeta \to \infty$, than do the secondary-flow velocities. The influence of Mach number and wall temperature on the corner layer is also evident in these figures. As in the case of the two-dimensional boundary layer, increasing the Mach number or heating the wall also thickens the corner layer. Figure 7 shows the streamwise velocity isovels. The effect of Mach number and wall temperature are also depicted.

The skin-friction coefficient distributions as given in figure 8 show a monotonic increase toward the asymptotic two-dimensional value. There are no overshoots in the skin friction (or heat transfer) similar to those found experimentally, and theoretically, for the hypersonic interaction in the corner (see Rubin & Lin 1972). It is probable that the hypersonic corner interaction, with the appearance of

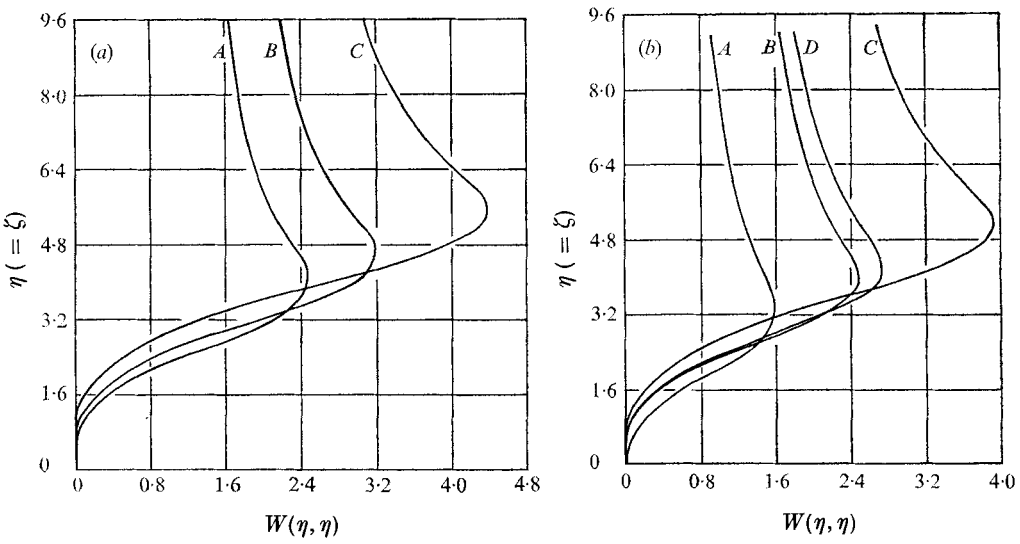

FIGURE 6. Secondary velocity along symmetry line: (*a*) adiabatic, (*b*) cold wall ($T_w/T_{stag} = 0{\cdot}6$)

		A	*B*	*C*		*A*	*B*	*C*	*D*
M_∞		0	0·95	1·50		0	0	2·0	1·5
T_w	(*a*)	1·0	1·18	1·45	(*b*)	0·6	1·0	1·08	0·87
χ		−2·5	−3·0	−5·0		−0·9	−2·5	−4·5	−2·5

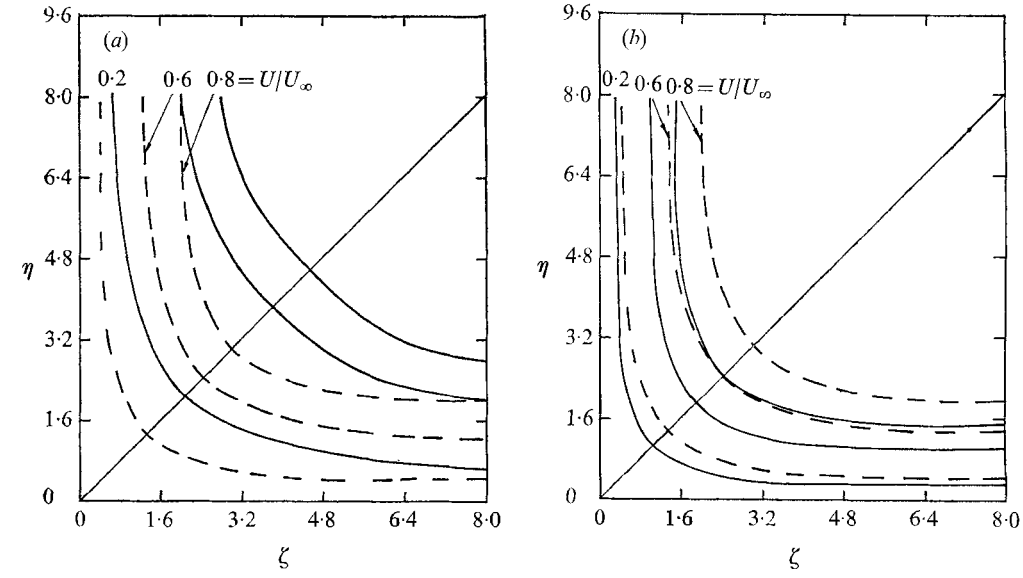

FIGURE 7. Streamwise isovels: (*a*) adiabatic, (*b*) cold wall ($T_w/T_{stag} = 0{\cdot}6$).

		M_∞	T_w	χ		M_∞	T_w	χ
– – – –	(*a*)	0	1·0	−2·5	(*b*)	0	1·0	−2·5
———		1·5	1·45	−5·0		0	0·6	−0·9

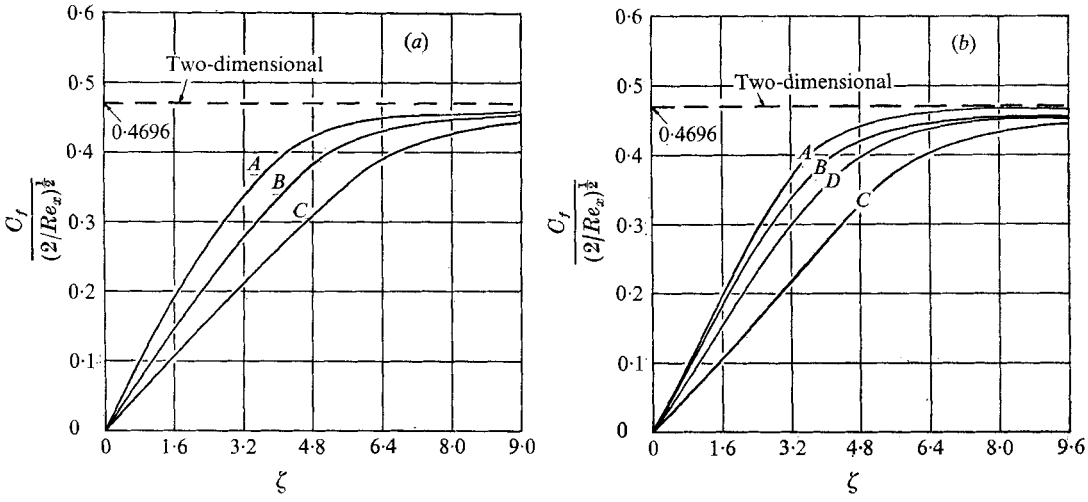

FIGURE 8. Skin-friction coefficient: (*a*) adiabatic, (*b*) cold wall ($I_w/I_{stag} = 0{\cdot}6$).

		A	*B*	*C*		*A*	*B*	*C*	*D*
M_∞	(*a*)	0	0·95	1·50	(*b*)	0	0	2·0	1·5
T_w	(*a*)	1·0	1·18	1·45	(*b*)	0·6	1·0	1·08	0·87
χ		−2·5	−3·0	−5·0		−0·9	−2·5	−4·5	−2·5

complex shock patterns associated with viscous–inviscid interaction, leads to these overshoots.

From the present analysis, overshoots in the skin-friction coefficient cannot be completely ruled out for colder walls and higher Mach numbers. From the asymptotic behaviour of the skin-friction coefficient it is found that, for positive values of χ, the asymptotic two-dimensional value will be approached from above.

$$\frac{C_f}{(2/Re\,x)^{\frac{1}{2}}} \sim f''(0)\left\{1+\frac{\chi}{\zeta^2}\right\}+O(\zeta^{-3}).$$

From figure 4 it would appear that, with colder wall boundary values, the constant χ tends to increase and should pass through zero. With $\chi > 0$, overshoots in C_f will occur.

Finally, a swirling motion is observed in the corner layer, but a closed vortical pattern is not established. The effect of raising the Mach number is to accentuate the swirling motion by increasing the cross-flow velocities which penetrate deeper into the corner layer. Cold wall calculations show that the swirl is diminished.

The research was supported by the Air Force Office of Scientific Research under grant 70–1843 and Modification 70–1843A, project 9781–01. The work reported here was based on part of a dissertation submitted by B. C. W. to the faculty of the Polytechnic Institute of Brooklyn in partial fulfillment of the requirements for the degree of Doctor of Philosophy (Aeronautics and Astronautics), 1972.

REFERENCES

BLOOM, M. H. 1966 Remark on compressibility effects in the boundary-layer cross-flow near a corner. *Polytechnic Institute of Brooklyn, PIBAL Rep.* no. 969.

BLOOM, M. H. & RUBIN, S. G. 1961 High-speed viscous corner flow. *J. Aero. Sci.* **28**, 145–157.

BLOOM, M. H., RUBIN, S. G. & CRESCI, R. J. 1970 Three-dimensional viscous interactions. *Proc. Symp. Viscous Interaction Phenomena in Supersonic and Hypersonic Flows*, pp. 493–511. Dayton University Press.

LIBBY, P. A. 1966 Secondary flows associated with a supersonic corner region. *A.I.A.A. J.* **4**, 1130–1132.

LIBBY, P. A. & FOX, H. 1963 Some perturbation solutions in laminar boundary-layer theory. Part 1. Momentum equation. *J. Fluid Mech.* **17**, 433–439.

PAL, A. & RUBIN, S. G. 1971 Asymptotic features of viscous flow along a corner. *Quart. Appl. Math.* **29**, 91–108.

PEACEMAN, D. W. & RACHFORD, H. H. 1955 The numerical solution of parabolic and elliptic differential equations. *J. Soc. Indust. Appl. Math.* **3**, 28–41.

RUBIN, S. G. 1966 Incompressible flow along a corner. *J. Fluid Mech.* **26**, 97–110.

RUBIN, S. G. & GROSSMAN, B. 1971 Viscous flow along a corner. Part 2. Numerical solution of corner-layer equations. *Quart. Appl. Math.* **29**, 169–186.

RUBIN, S. G. & LIN, T. C. 1972 Numerical methods for three-dimensional viscous flow problems. Application to the hypersonic leading edge. *J. Comp. Phys.* **9**, 339–364.

SMITH, G. D. 1965 *Numerical Solutions of Partial Differential Equations.* Oxford University Press.

STEWARTSON, K. 1964 *The Theory of Laminar Boundary Layers in Compressible Fluids.* Oxford University Press.

WEINBERG, B. C. 1972 Compressible corner flow. Ph.D. thesis, Polytechnic Institute of Brooklyn.